Cell Reports
Physical Science

CellPress
OPEN ACCESS

Article

Engineered living hydrogels for robust biocatalysis in pure organic solvents

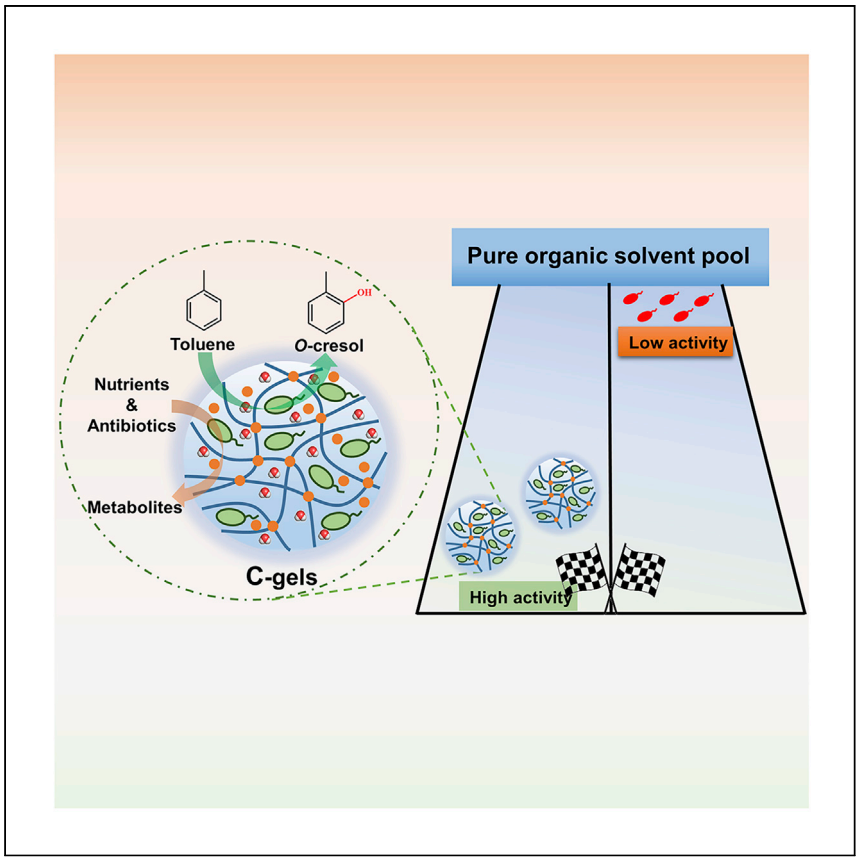

A versatile strategy to improve the organic solvent tolerance of whole-cell biocatalysts is highly demanded. Gao et al. design engineered living hydrogels using genetically modified microbial cells for improved organic solvent tolerance and robust biocatalysis in pure organic solvents.

Liang Gao, Lilin Feng, Daniel F. Sauer, Malte Wittwer, Yong Hu, Johannes Schiffels, Xin Li

yonghu@tongji.edu.cn (Y.H.)
j.schiffels@biotec.rwth-aachen.de (J.S.)
xli@dwi.rwth-aachen.de (X.L.)

Highlights

Living hydrogels are engineered by integrating microbial cells and alginate hydrogels

Hydrogel microenvironments modulate catalytic efficiency of engineered living hydrogels

Engineered living hydrogels enable improved solvent tolerance in pure organic solvents

The versatility of engineered living hydrogels for robust biocatalysis is verified

Gao et al., Cell Reports Physical Science 3, 101054
October 19, 2022 © 2022 The Author(s).
https://doi.org/10.1016/j.xcrp.2022.101054

Cell Reports
Physical Science

CellPress
OPEN ACCESS

Article

Engineered living hydrogels for robust biocatalysis in pure organic solvents

Liang Gao,[1,5] Lilin Feng,[1,2,5] Daniel F. Sauer,[1] Malte Wittwer,[1] Yong Hu,[3,*] Johannes Schiffels,[1,*] and Xin Li[2,4,6,*]

SUMMARY

Engineered living hydrogels that can protect cells from harsh environments have achieved preliminary successes in biomedicine and environmental remediation. However, their biocatalytic applications in pure organic solvents have not been explored. Here, living hydrogels were engineered by integrating genetically modified *Escherichia coli* cells into alginate hydrogels for robust biocatalysis in pure organic solvents. The biocompatible hydrogels could not only support cell growth and diminish cell escape but could also act as protective matrices to improve organic solvent tolerance, thereby prolonging catalytic activity of whole-cell biocatalysts. Moreover, the influence of hydrogel microenvironments on biocatalytic efficiency was thoroughly investigated. Importantly, the versatility of engineered living hydrogels paves the way to achieve robust biocatalytic efficiency in a variety of pure organic co-solvents. Overall, we are able to engineer living hydrogels for regio-selective synthesis in pure organic solvents, which may be particularly useful for the innovation of living hydrogels in biocatalysis.

INTRODUCTION

Chemo-, regio-, and stereo-selective synthesis has always been challenging. Nonetheless, the selective preparation of industrially relevant intermediates,[1] (chiral) drugs,[2] and food additives[3] is highly demanded by our daily life. Furthermore, selective synthesis of compounds significantly contributes to a green production process due to the reduction of byproducts and waste. Biocatalysts (e.g., enzymes) have inherent advantages in chemo-, regio-, and stereo-selectivity.[1,4] However, these biocatalysts often suffer from low tolerance to a high concentration of hydrophobic compounds (e.g., substrates or organic solvents), which diminishes their biocatalytic efficiency.[5] Therefore, whole-cell biocatalysts are adopted as a desired biocatalytic system for selective synthesis, which have individual compartments to protect inner enzymes.[6,7] In this precious work, we catalogized recent technologies for the integration of whole cells and artificial metalloenzymes that may create a novel biocatalytic pathway and achieve higher biocatalytic efficiency.[8] Nevertheless, the whole-cell biocatalysts are not universal and are often inactivated by a high concentration of organic solvent.[9,10] For instance, in the hydroxylation of monosubstituted benzenes (an important reaction in industry-relevant intermediates), whole-cell biocatalysts cannot achieve satisfactory catalytic activity because of considerable cytotoxicity of substrate.[11,12] Therefore, a versatile strategy to improve the organic solvent tolerance of biocatalysts is highly demanded.

[1]Institute of Biotechnology, RWTH Aachen University, 52074 Aachen, Germany

[2]DWI-Leibniz-Institute for Interactive Materials e.V., 52056 Aachen, Germany

[3]Department of Polymeric Materials, School of Materials Science and Engineering, Tongji University, Shanghai 201804, China

[4]Institute for Technical and Macromolecular Chemistry, RWTH Aachen University, 52074 Aachen, Germany

[5]These authors contributed equally

[6]Lead contact

*Correspondence: yonghu@tongji.edu.cn (Y.H.), j.schiffels@biotec.rwth-aachen.de (J.S.), xli@dwi.rwth-aachen.de (X.L.)

https://doi.org/10.1016/j.xcrp.2022.101054

This is an open access article under the CC BY-NC-ND license (http://creativecommons.org/licenses/by-nc-nd/4.0/).

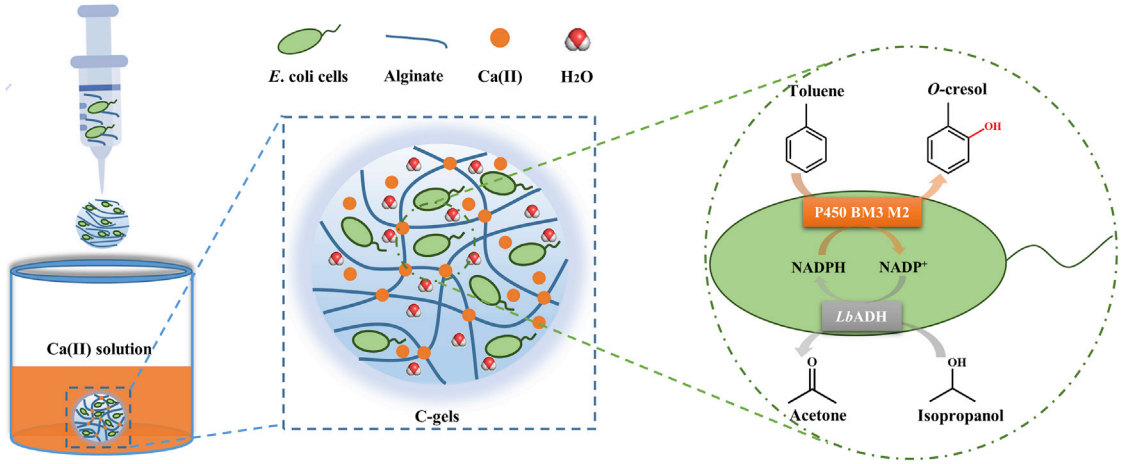

Figure 1. Schematic illustration of the engineered C-gels for the conversion of toluene to *o*-cresol by genetically modified *E. coli* cells containing P450 BM3 M2 and *Lb*ADH

Isopropanol was used as co-substrate of *Lb*ADH for NADP(H) co-factor regeneration.

Engineered living materials are acknowledged as the most relevant contemporary revolution in the fields of materials science and engineering and which can outperform the existing multifunctional materials including intelligent or bioactive materials toward real-word applications.[13–16] Given the particular importance, the European Union Commission recently launched the EIC Pathfinder Challenge on engineered living materials to promote the researcher's exploration at the forefront of the emerging field.[17] In practice, microbial cells are widely employed as living components due to their responsiveness to environmental stimuli and adjustable cell programming through gene editing.[18,19] On the other hand, hydrogels have attracted great attention in various applications because of their high water content, three-dimensional (3D) cross-linked network, chemical diversity, and stimulus responsiveness.[20–24] In particular, the biocompatible and biodegradable hydrogels are adopted to integrate living microbial cells, which breeds a nascent field of engineered living hydrogels.[25] In virtue of their unique properties, hydrogels can meet the stringent requirements for the design of engineered living hydrogels.[26–28] For instance, the biochemical permeability of hydrogels supports normal metabolic function of living microbial cells.[29] Likewise, the architectural characteristics of hydrogels can spatially confine living microbial cells[30] while protecting cells against harsh environment.[31] Notably, in these systems, living microbial cells endow hydrogels with engineered functions, and hydrogel microenvironments, in turn, can modulate cell behaviors.[32] Although the engineered living hydrogels have been successfully applied in biomedicine and environment, they remain unexplored in the general field of biocatalysis so far.

Herein, the living hydrogels are engineered by integrating genetically modified *Escherichia coli* (*E. coli*) whole cells for *o*-hydroxylation of monosubstituted benzenes in neat substrate or pure organic co-solvents (Figure 1). The biocompatible hydrogel matrices are capable of sustaining cell growth, diminishing cell escape, and improving organic solvent tolerance, thus prolonging cell activity in neat substrate. Additionally, hydrogel microenvironments, including water content, calcium ion (Ca(II)) concentration, and network hydrophobicity, are able to further adjust the regio-selective catalytic efficiency. Compared with free cells in toluene, the engineered living hydrogels display about 8 times higher catalytic rate within 4 h and a 2.7 times higher amount of product *o*-cresol. Moreover, the improved organic solvent tolerance and regio-selective biocatalysis of engineered living hydrogels are

observed in pure organic co-solvents with the log p of more than 2.7 or the organic co-solvent of methyl *tert*-butyl ether (MTBE).

RESULTS AND DISCUSSION

Engineering of living hydrogels

Alginate, a natural polysaccharide, is commercially available and cost effective.[33] It can be employed to prepare the biocompatible hydrogels by the facile and mild method for biomedical applications.[34,35] To integrate living whole cells into alginate hydrogels, *E. coli* cells were suspended in the alginate solution and then added dropwise to Ca(II) solution via a syringe to obtain the engineered living hydrogels (C-gels) by ionic cross-linking. Through adjusting the concentration of Ca(II) solution, we found that concentrations ranging from 0.15% (m/v) to 1% (m/v) are ideal for obtaining the intact and stable architectures of C-gels. Clearly, single C-gel exhibited a mean diameter of about 2.0 mm (Figure 2A) and water content of around 92.6% (m/m) (Table S1) and could accommodate about of 2.9×10^8 cells (Table S2). The microstructure of the fresh C-gel was observed by cryo-scanning electron microscopy (cryo-SEM) imaging (Figure 2B). The C-gel displayed a typical 3D cross-linked network with a pore size of around 5–15 μm. Meanwhile, the growth of cells in the C-gels was then surveyed (Figure 2C). Apparently, the growth rate of cells in hydrogel matrices was similar to that of free cells in the medium. This is attributed to the biocompatibility of hydrogel matrices and the hydrated microenvironment of hydrogels that allows for the diffusion of nutrients, antibiotics, and metabolites.

Moreover, the confinement of cells by hydrogels with different cross-linking degrees was assessed (Figure 2D). The C-gels prepared at a low Ca(II) concentration (0.15%) showed the escape of cells to the surrounding medium at the first test point (2 h). In contrast, no cell escape was observed for the C-gels prepared at a high Ca(II) concentration (1.0%) even after 4 h. These results suggested that the C-gels with a high Ca(II)-cross-linking degree can diminish the cell escape.

Next, wild-type *E. coli* cells were genetically modified to co-express *Lactobacillus brevis* alcohol dehydrogenase (*Lb*ADH) and P450 BM3 M2. These genetically modified cells are capable of performing the industrially relevant hydroxylation of monosubstituted benzenes. The biocatalytic mechanism is that the engineered P450 BM3 variant M2 (R47S/Y51W/I401M) can produce *o*-substituted phenols (i.e., from toluene to *o*-cresol) by forming epoxide intermediate and NIH shifting of a methyl group at room temperature in the presence of oxygen and NADP(H) co-factor.[11,37,38] In order to obtain the strain with efficient catalytic properties, NADP(H)-dependent *Lb*ADH gene was introduced into the same strain and co-expressed P450 BM3 M2 for NADP(H) recycling (Figure 1). The co-expression of *Lb*ADH and P450 BM3 M2 within genetically modified cells was verified by SDS-PAGE (Figure S1) and CO difference spectroscopy (Figure S2). Furthermore, the biocatalytic capability of genetically modified cells (also termed as free cells) was investigated by the hydroxylation of toluene to *o*-cresol (Figure 2F). The generated *o*-cresol was detected by gas chromatograph (Figure S3). After the addition of co-substrate isopropanol, the amount of *o*-cresol produced by free cells co-expressed of P450 BM3 and *Lb*ADH was obviously higher than that produced by free cells containing P450 BM3 M2 alone, demonstrating that the co-expressed *Lb*ADH contributed to the successful generation of an efficient cofactor (NADP(H)) regeneration system. Subsequently, the cell activity of integrated C-gels was also examined using 7-benzoxy-3-carboxycoumarin ethyl ester (BCCE) assay (Figures 2E and S4).[36] Delightfully, a large area of blue fluorescence (7-hydroxycoumarin-3-carboxylic

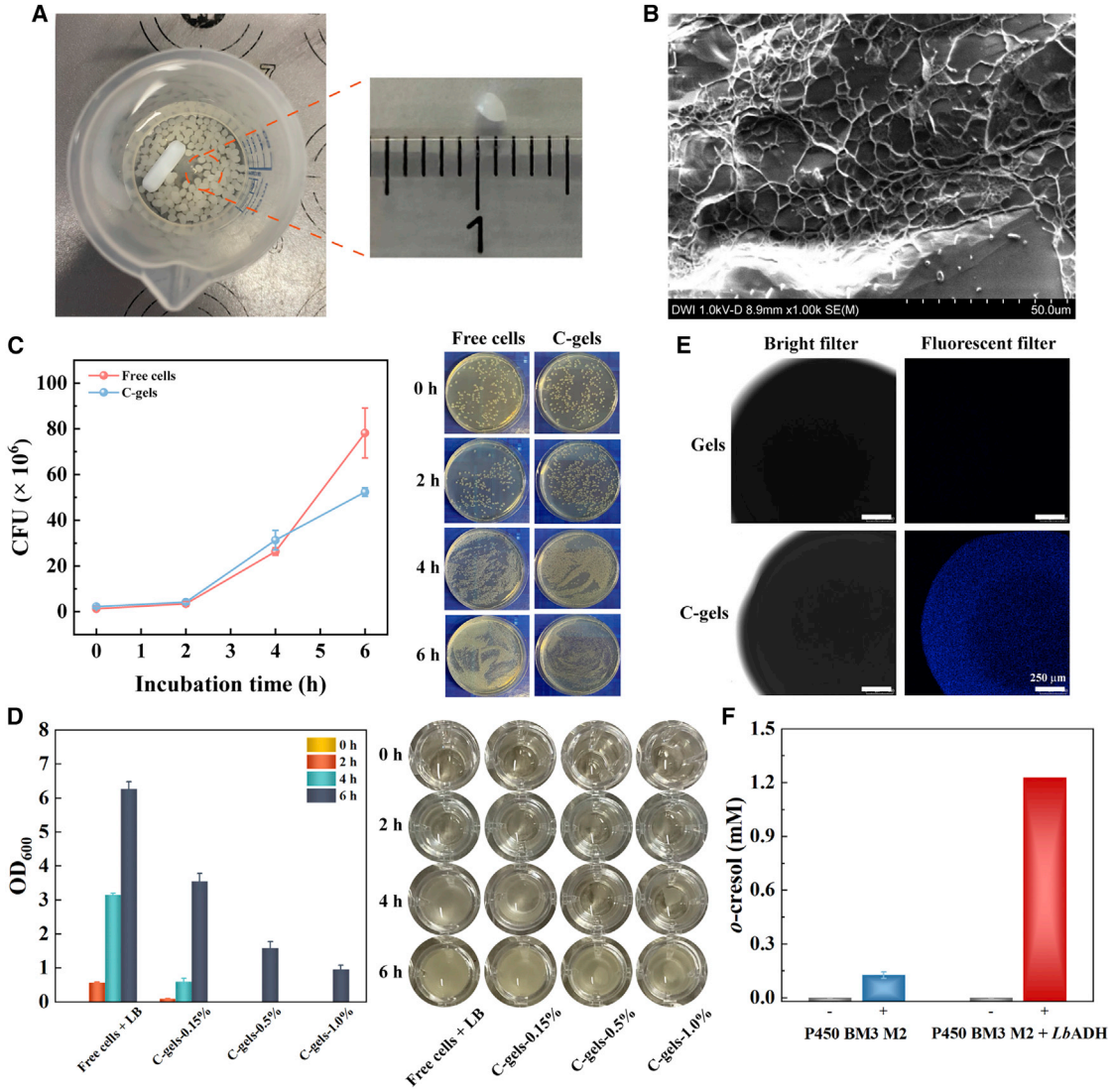

Figure 2. Preparation and characterization of engineered living hydrogels for cell growth, escape, and biocatalysis

(A and B) Digital photo (A) and cryo-SEM image (B) of the C-gels.

(C) Growth curve and photo of *E. coli* cells in medium and hydrogel matrices (n = 3; error bars represent the standard deviation).

(D) Confinement of cells by hydrogels with different Ca(II)-cross-linking degrees (n = 3; error bars represent the standard deviation).

(E) Confocal microscopic images of hydrogels and C-gels after BCCE activity test. The blue fluorescence was generated with *o*-dealkylation of BCCE by living cells containing P450 BM3 M2 and *Lb*ADH.[36]

(F) The amount of *o*-cresol produced by free cells containing P450 BM3 M2 alone or co-expressed P450 BM3 M2 and *Lb*ADH (n = 2; error bars represent the standard deviation). −: no addition of isopropanol; +: with addition of isopropanol.

acid) produced by living cells was observed, suggesting that the engineered C-gels have an excellent cell activity.

Biocatalytic activities of C-gels in neat substrate

To assess organic solvent tolerance of C-gels, highly toxic toluene was chosen as substrate and likewise as reaction solvent. Naturally, *E. coli* cells prefer aqueous medium, and hence the hydrated microenvironment is crucial to achieve effective catalysis. Firstly, the effect of aqueous buffer content on biocatalytic efficiency of free cells and C-gels was investigated (Figure 3A). For free cells, 1.56 mM *o*-cresol was produced in neat toluene without the addition of buffer. By increasing the buffer content, the product

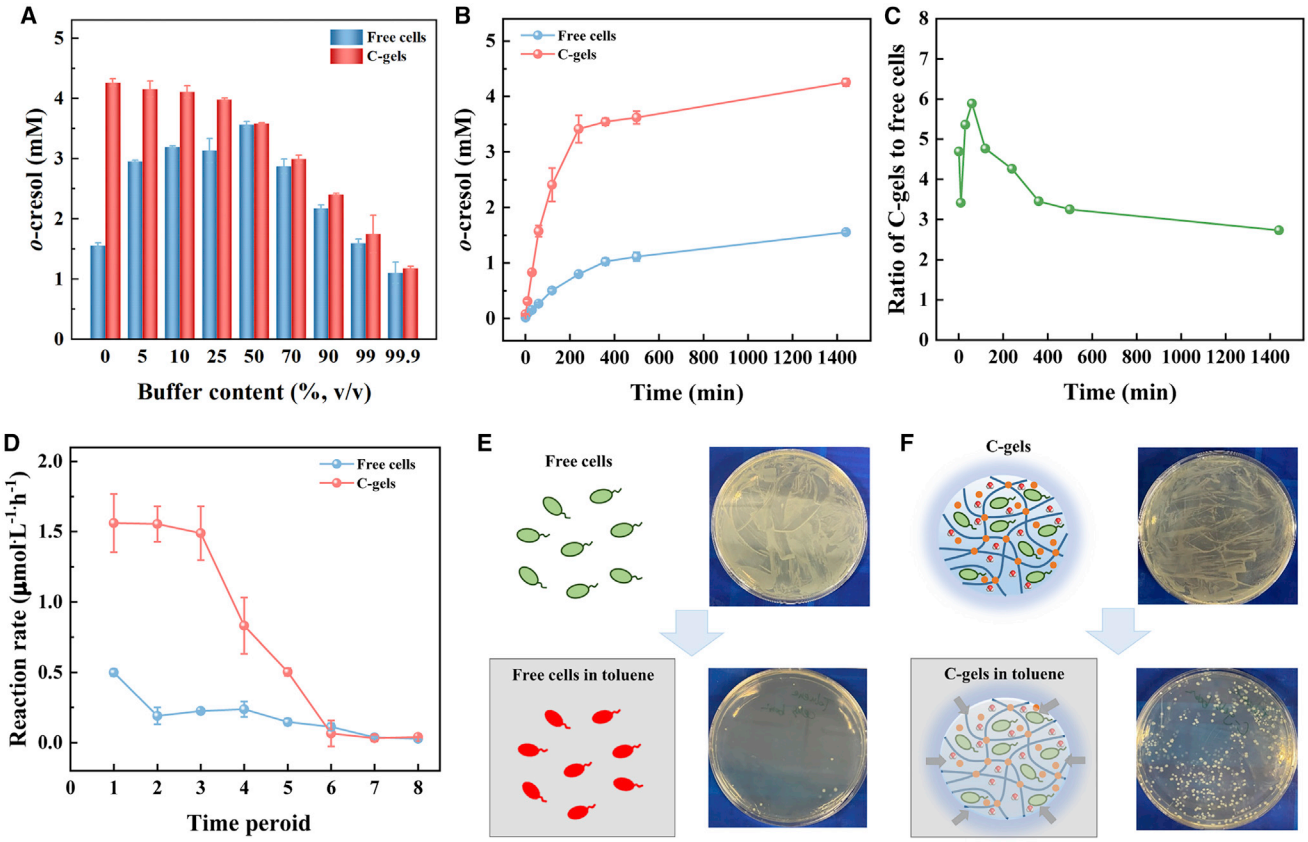

Figure 3. Biocatalytic efficiency and cell viability of free cells and C-gels in neat toluene

(A) The amount of *o*-cresol produced by free cells and C-gels at different buffer contents (n = 3; error bars represent the standard deviation).

(B) Time course of biocatalysis for free cells and C-gels in neat toluene (n = 3; error bars represent the standard deviation).

(C) Product ratio of C-gels to free cells in neat toluene at different time points.

(D) Corresponding catalysis rate for free cells and C-gels in neat toluene (n = 3; error bars represent the standard deviation). Time periods: 1 (1–10 min), 2 (10–30 min), 3 (30–60 min), 4 (60–120 min), 5 (120–240 min), 6 (240–360 min), 7 (360–500 min), and 8 (500–1,440 min).

(E and F) Cell activity assay of (E) free cells and (F) C-gels before and after soaking with neat toluene.

amount reached the highest amount of 3.56 mM at 50% buffer content and then decreased. Therefore, the catalytic efficiency of free cells can be improved at an appropriate content of aqueous medium, but the formed organic/aqueous biphasic system still remains challenging for downstream separation.[5] In contrast, 2.7-fold more product was obtained from C-gels than from free cells in neat toluene. Notably, the product amount decreased with increased buffer content for C-gels. This may be due to the fact that the aqueous content of hydrogels has already met the demand of cell catalysis, and an excessive water content was not helpful for improving catalytic efficiency. These results suggested that the hydrated microenvironment of hydrogels is favorable for enhancing whole-cell catalysis in neat toluene.

In order to deeply study the efficiency of the C-gels in neat toluene, the catalytic property of biocatalyst in neat toluene over time was firstly explored under optimized reaction conditions, such as shaking with 1,100 RPM and the addition of 20 mM isopropanol (Figures S5 and S6). Apparently, the amount of *o*-cresol produced by C-gels was higher than that produced by free cells over the whole time period (Figure 3B). Meanwhile, the obvious turning point of product amount from C-gels came out at 4 h because the long-term penetration damage from toluene deactivated C-gels. Nevertheless, the maximum product ratio of C-gels to free cells

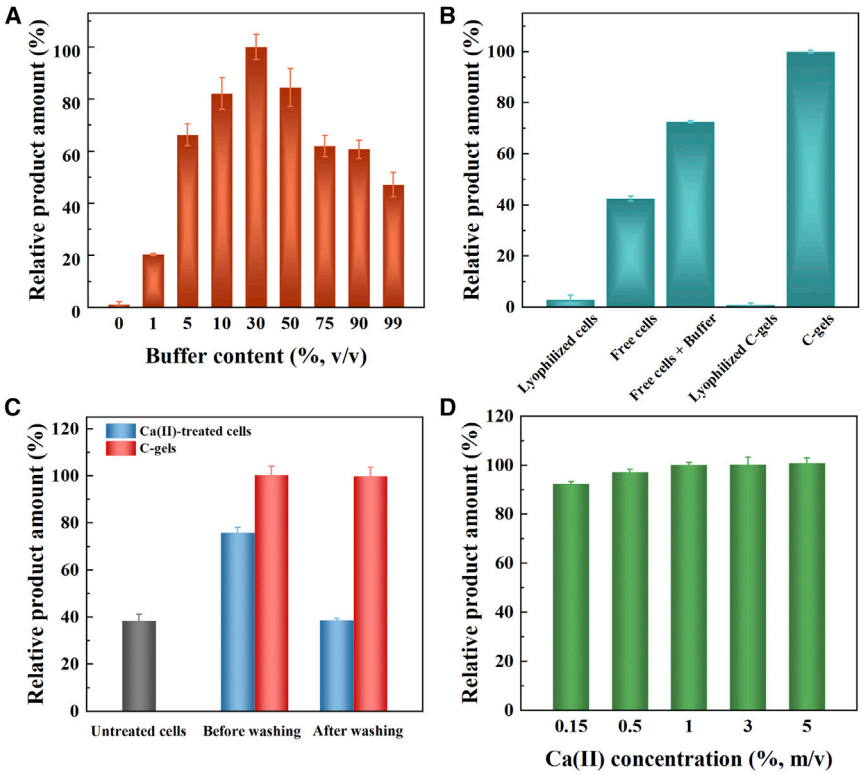

Figure 4. Biocatalytic efficiency of C-gels under different hydrogel microenvironments

(A) Influence of additional buffer content on the biocatalytic efficiency of lyophilized C-gels in neat toluene (n = 3; error bars represent the standard deviation).

(B) Comparation of biocatalytic efficiency of free cells in buffer-containing biphasic system and C-gels in neat toluene (n = 3; error bars represent the standard deviation).

(C) Influence of washing steps on the production of *o*-cresol by Ca(II)-treated cells or C-gels (n = 3; error bars represent the standard deviation).

(D) Influence of Ca(II) concentration on the production of *o*-cresol by C-gels (n = 3; error bars represent the standard deviation).

reached 5.9-fold at 60 min (Figure 3C). Likewise, compared with free cells, C-gels exhibited higher catalytic efficiency within 240 min and were even able to maintain a high catalytic rate of 1.5 $\mu mol \cdot L^{-1} \cdot h^{-1}$ for the first 60 min (Figure 3D), indicating that the initial high and stable activity of C-gels contributed to the high productivity. Additionally, after soaking with neat toluene for 1 h, free cells were completely inactivated, while C-gels still maintained cell viability (Figures 3E and 3F). These results demonstrated that with the protective effect of hydrogel matrices, the engineered C-gels display superior organic solvent tolerance and can protect cells from toxic toluene, thus prolonging the catalytic efficiency of C-gels in neat substrate.

Influence of hydrogel microenvironments on biocatalytic efficiency

The alginate hydrogel matrices contain highly organized 3D network structure, which is controlled significantly by aqueous solution and cross-linker (Ca(II)). Therefore, the influence of hydrogel microenvironments (e.g., water content, Ca(II) concentration, and network hydrophobicity) on biocatalytic activity was investigated. Firstly, to reveal the importance of inner aqueous microenvironment, the biocatalytic efficiency of lyophilized C-gels at different contents of aqueous buffer was tested (Figure 4A). The lyophilized C-gels without buffer content showed almost no catalytic ability in neat toluene. As the buffer content increases, the *o*-cresol amount firstly increased and then decreased,

and the highest product amount was obtained at a buffer content of 30% (v/v). Notably, each lyophilized C-gel can absorb more than 2.5 mg of the aqueous amount in the supplement buffer content of 30% (v/v). In other words, the water content of hydrated lyophilized C-gels reaches to the level of freshly prepared C-gels (92.6%; Table S1). These results indicated that the internal water content of the freshly prepared hydrogels is vital to achieve an optimal biocatalytic activity in neat substrate. Secondly, compared with free cells with buffer, C-gels exhibited a higher product amount under neat toluene (Figure 4B), suggesting that the hydrogels can also serve as a protective matrix to further improve the biocatalytic efficiency in neat substrate. Thirdly, the hydrophobic ligand (amylamine or 2-phenethylamine) grafted alginates were employed to increase the hydrophobicity of gel network (Figure S7A). By nuclear magnetic resonance (NMR) integration, the content of amylamine or 2-phenethylamine grafted to alginate was calculated to be about 33%. As expected, a significantly reduced biocatalytic efficiency was observed in the hydrophobically modified C-gels (Figure S7B). This is due to the introduction of hydrophobic ligands altering the aqueous microenvironment in hydrogels.

Finally, the influence of Ca(II) concentration on the catalytic efficiency of free cells and C-gels was evaluated. After free cells were treated with Ca(II) solution, they produced a higher amount of *o*-cresol than untreated cells in neat substrate, and the product amount increased with the Ca(II) concentrations (Figure S8). This is attributed to the formation of a compact and rigid cell membrane through Ca(II)-mediated cross-linking of lipopolysaccharide (LPS) in the extracellular matrix, resulting in the improved organic solvent tolerance and biocatalytic efficiency.[39,40] However, when Ca(II)-treated cells underwent a washing step, their product amount reduced to the level of untreated cells (Figure 4C) due to the loss of Ca(II) from the cell surface and surrounding microenvironment. Remarkably, cells in the Ca(II)-cross-linked hydrogel network produced a higher product amount (100%) than Ca(II)-treated cells (76%) in neat toluene. More importantly, the biocatalytic efficiency of C-gels did not decrease after washing steps due to the stable coordination of Ca(II) ions in the hydrogel network.

Furthermore, the biocatalytic efficiency of C-gels with different Ca(II) concentrations in hydrogel network was investigated (Figure 4D). While the increased product amount was observed at the higher Ca(II) concentrations, C-gels displayed a high product formation (>92.3%) at the Ca(II) concentration as low as 0.15% (m/v). Such stable biocatalytic activity indicated that Ca(II) ions are not only crucial for the formation of hydrogels but also beneficial for maintaining biocatalytic efficiency of C-gels in neat toluene. Overall, hydrogel microenvironments, including water content, Ca(II) concentration, and network hydrophobicity, play key roles in adjusting biocatalytic efficiency of C-gels.

Organic co-solvent tolerance of C-gels

Next, the versatility of C-gels for improved solvent tolerance and biocatalytic efficiency was studied in different organic co-solvents, with a broad range of log p values. Normally, water-insoluble substrates need to be dissolved in organic co-solvent to obtain a high concentration of substrate. Therefore, biocatalysis in pure organic co-solvents will undoubtedly enhance the substrate solubility and stability, as well as simplify the downstream separation process and even improve the catalyst selectivity.[5] When the log p of organic co-solvents was less than 2.3, both free cells and C-gels showed very low biocatalytic efficiency (Figure 5A). The exceptional example is that C-gels displayed a higher biocatalytic efficiency than free cells in the organic co-solvent of MTBE.[41–44] Likewise, C-gels also displayed a higher product amount in other organic co-solvents with a log p above 2.7. These results suggested that the engineered C-gels can indeed improve the biocatalytic efficiency

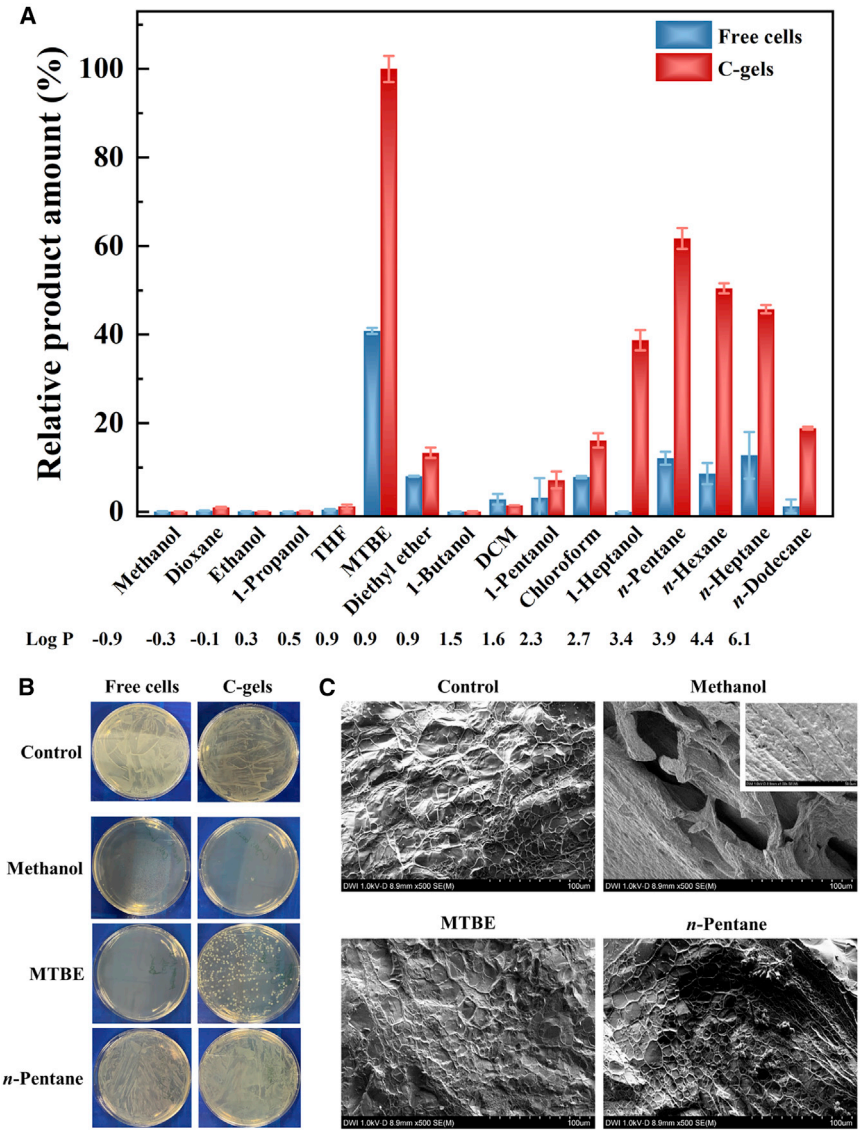

Figure 5. Biocatalytic efficiency and cell viability of free cells and C-gels in varied pure organic co-solvents

(A) Biocatalysis of free cells and C-gels in different organic co-solvents containing 10% (v/v) toluene (n = 3; error bars represent the standard deviation).

(B) Cell activity assay of free cells and C-gels before and after soaking with the organic co-solvents with different log p.

(C) Cryo-SEM images of C-gels after soaking with the organic co-solvents with different log p. Log p: the logarithm of partitioning coefficient of a solvent in a defined *n*-octanol-water mixture.

in a variety of organic co-solvents. To better understand the interaction between C-gels and organic co-solvents, the transmutation of hydrogel structure and the bioactivity of cells under the representative organic co-solvents with different log p were investigated, i.e., methanol (log p = −0.9), MTBE (log p = 0.9), and *n*-pentane (log p = 3.4) (Figures 5B and 5C). Clearly, after soaking with methanol, both free cells and C-gels were completely inactivated, and the hydrogel network collapsed. This was attributed to the fact that methanol could rapidly penetrate into the hydrogel network and alter the interaction between alginate and calcium ions. As a comparison, after soaking with MTBE, free cells were inactivated, whereas C-gels still

maintained cell viability, and their hydrogel network was also intact. Notably, after soaking with *n*-pentane, both free cells and C-gels displayed high cell activity, and the hydrogel network also remained intact, suggesting that the cytotoxicity of *n*-pentane is minimal and that the hydrophobicity limits its penetration within the hydrogel network. However, the final low biocatalytic efficiency of free cells in the organic co-solvent of *n*-pentane was entirely attributable to the prolonged penetration of highly toxic toluene. These results again demonstrated that the hydrogel matrix as a protective shell can improve their organic solvent tolerance and enhance the catalytic efficiency. However, a bottleneck is that high cell viability is more favorable in the organic co-solvents with high log p, yet these organic co-solvents may in turn impede the transportation of preferred substances to the catalyst active center.

In summary, we engineered living hydrogels with improved organic solvent tolerance for robust biocatalysis in neat substrate or pure organic co-solvents. The biocompatible hydrogel matrices with high aqueous content allow for the diffusion of nutrients and metabolites through the network to sustain cell growth. Likewise, hydrogel matrices can also diminish cell escape and improve organic solvent tolerance and thus prolong cell activity in neat substrate. Moreover, hydrogel microenvironments, such as water content, Ca(II) concentration, and network hydrophobicity, are able to adjust the biocatalytic efficiency. More importantly, the versatility of engineered living hydrogels paves the way for biocatalysts to obtain higher catalytic activity in a variety of pure organic co-solvents. According to our extensive literature survey, this is the first example to demonstrate the use of engineered living hydrogels for improved regio-selective biocatalysis in *o*-hydroxylation of monosubstituted benzenes.

This study may mark the beginning of a new field of engineered living hydrogels for biocatalysis in pure organic solvents. In the future, we will focus on optimizing the interactions between living cells and hydrogels and explore the relationship between hydrogel microenvironment and cell function of engineered living hydrogels. Moreover, hydrogels with multilayered core/shell structures should be constructed to protect the cells from insults of organic solvents in a controlled manner, thereby further improving biocatalytic efficiency in pure organic solvents. We believe that the engineered living hydrogels as "compatibilizers" can be employed to facilitate the mixing of incompatible liquids in the hydrogel network and are expected to address the contradiction between insoluble substrates and aqueous favorable biocatalysts.

EXPERIMENTAL PROCEDURES

Resource availability

Lead contact

Further information and requests for resources and reagents should be directed to and will be fulfilled by the lead contact, Xin Li (xli@dwi.rwth-aachen.de).

Materials availability

This study did not generate new unique reagents.

Data and code availability

All data supporting the findings of this study are available within the article and are described in the supplemental information or are available from the lead contact upon reasonable request. This study did not generate/analyze datasets/code.

Preparation of C-gels

E. coli cells (OD_{600} = 40, 5 mL) were centrifuged and resuspended in alginate solution (1% [m/v], 5 mL, 50 mM 4-(2-hydroxyethyl)-1-piperazineethanesulfonic acid

[HEPES] [pH 7.0]). C-gels were achieved through dropping the cell-alginate mixture into $CaCl_2 \cdot 2H_2O$ solution (1% [m/v], 25 mL) using the syringe (needle's diameter: 0.6 mm) with stirring (350 RPM). The C-gels were collected and washed three times using HEPES buffer (50 mM, pH 7.0).[45] Subsequently, the amount of C-gels beads was counted. Varied Ca(II) concentrations (0.15%, 0.5%, 1%, 3%, 5% [m/v]) were set up to study effect of Ca(II) on *o*-cresol production using C-gels. C-gels (11 beads, corresponding to free cells [200 μL, OD_{600} = 20]) were transferred into the reactor (1.5 mL GC glass vial), and the rest of the free liquid in the reactor was gotten rid of by pipetting. For free cells (200 μL, OD_{600} = 20) in the GC vial, the aqueous solution was piped away after centrifugation (4,000 RPM, 4°C, 15 min).

Growth of cells in hydrogel beads

To test the growth of bacteria in alginate hydrogel bead, one bead containing encapsulated cells under 1% (m/v) $CaCl_2 \cdot 2H_2O$ (approx. 3.5×10^6 cells per bead) was transferred into one well and incubated in LB medium (200 μL, 50 μg/mL kanamycin) using 96-well microtiter plates (37°C, 900 RPM, 70% humidity). The bead was retrieved at a certain time point by washing three times with HEPES buffer (200 μL, 50 mM, pH 7.0). Afterward, the bead was transferred into sodium citrate solution (55 mM, 1 mL) and dissolved totally through shaking (1 min). The above solution (1 μL) was further diluted into HEPES buffer (1 mL, 50 mM, pH 7.0). Finally, 100 μL solution was plated on an LB agar plate (50 mg/mL kanamycin) and incubated overnight (37°C). The clones were subsequently counted for calculation of the cell amount in the hydrogel bead at time points of 0, 2, 4, and 6 h. Non-encapsulated cells (starting OD_{600} = 0.022, approx. 3.5×10^6 cells per well) incubated in LB medium were set up as control. All samples were prepared independently with triplication.

Cell escape from hydrogel beads

E. coli cells, containing empty vector pET28a, were pre-cultured in LB medium (10 mL, 50 μg/mL kanamycin) using a 25 mL flask (37°C, 200 RPM) overnight. The cells were then collected by centrifugation (11,000 RPM, 1 min). The cell pellet was washed once, resuspended with HEPES buffer (4 mL, 50 mM, pH 7.0), and stored on ice for further use.

E. coli cells (OD_{600} = 20, 20 μL) were centrifuged and resuspended in alginate solution (1% [m/v], 2 mL, 50 mM HEPES [pH 7.0]). C-gels were achieved through dropping the cell-alginate mixture into $CaCl_2 \cdot 2H_2O$ solution (0.15%, 0.5%, or 1% [m/v], 25 mL) using the syringe (needle's diameter: 0.6 mm) with stirring (350 RPM). The beads formed under different Ca(II) concentrations were collected and washed three times using HEPES buffer (25 mL, 50 mM, pH 7.0), respectively. One bead containing encapsulated cells under 0.15%–1% (m/v) $CaCl_2 \cdot 2H_2O$ (approx. 3.5×10^6 cells per bead) was transferred into one well, respectively, and incubated in LB medium (200 μL, 50 μg/mL kanamycin) using 96-well microtiter plates (37°C, 900 RPM, 70% humidity). The cell density in the LB medium was detected (values of OD_{600}) at certain time points (0, 2, 4, and 6 h) using non-encapsulated cells as control. All samples were prepared independently with triplication.

Conversion of toluene to *o*-cresol using free cells and C-gels

The reaction mixture (200 μL) consisting of HEPES buffer (50 mM, pH 7.0), toluene, and isopropanol was supplied into the GC vial containing free cells or C-gels to start the reaction under shaking (1,100 RPM, 25°C, 24 h). In order to investigate the isopropanol affection on biocatalysis, different isopropanol concentrations (20–1,000 mM) were applied in the reaction mixture to check the final *o*-cresol concentration.

For reactions under neat toluene, the HEPES buffer was excluded in the reaction mixture. Moreover, whether mechanical shaking (11,000 RPM) or magnetic stirring (500 RPM) affect the *o*-cresol production for non-encapsulated free cells and C-gels was investigated under neat toluene. The *o*-cresol concentration (4.26 mM) of C-gels was set as 100% for comparison with that of non-encapsulated free cells. For the reaction using cells encapsulated in hydrophobic ligands modified alginate hydrogels, the biocatalytic process was performed for 24 h under neat toluene, and the *o*-cresol concentration (4.26 mM) from C-gels (no modified alginate) was set as 100%. In case of organic co-solvents affection, 16 different solvents with different log p values were selected for toluene conversion using non-encapsulated free cells and C-gels. The *o*-cresol concentration (1.52 mM) from C-gels under pure MTBE was set as 100%. See the supplemental experimental procedures for further information.

SUPPLEMENTAL INFORMATION

Supplemental information can be found online at https://doi.org/10.1016/j.xcrp.2022.101054.

ACKNOWLEDGMENTS

This research was funded by the National Natural Science Foundation of China (52103181), Sino-German Center for Research Promotion (GZ1505), and Fundamental Research Funds for the Central Universities (22120210364). L.G. and L.F. are supported by the China Scholarship Council (CSC nos. 201708330280 and 201708330279).

AUTHOR CONTRIBUTIONS

L.G., J.S., and X.L. provided the experiment design; L.G. and L.F. performed all experiments; L.G., L.F., D.F.S., M.W., J.S., and X.L. analyzed the data; L.G., D.F.S., Y.H., and X.L. wrote the manuscript. All authors discussed the results and revised the manuscript. All authors approved the final version of the manuscript.

DECLARATION OF INTERESTS

The authors declare no competing interests.

Received: April 15, 2022
Revised: August 5, 2022
Accepted: August 22, 2022
Published: September 12, 2022

REFERENCES

1. Wu, S., Snajdrova, R., Moore, J.C., Baldenius, K., and Bornscheuer, U.T. (2021). Biocatalysis: enzymatic synthesis for industrial applications. Angew. Chem. Int. Ed. Engl. *60*, 88–119. https://doi.org/10.1002/anie.202006648.

2. Taylor, D. (2015). The pharmaceutical industry and the future of drug development. Pharm. Environ. *1-33*, 1–33. https://doi.org/10.1039/9781782622345-00001.

3. Carocho, M., Barreiro, M.F., Morales, P., and Ferreira, I.C.F.R. (2014). Adding molecules to food, pros and cons: a review on synthetic and natural food additives. Compr. Rev. Food Sci. Food Saf. *13*, 377–399. https://doi.org/10.1111/1541-4337.12065.

4. Hauer, B. (2020). Embracing nature's catalysts: a viewpoint on the future of biocatalysis. ACS Catal. *10*, 8418–8427. https://doi.org/10.1021/acscatal.0c01708.

5. Schmid, A., Dordick, J.S., Hauer, B., Kiener, A., Wubbolts, M., and Witholt, B. (2001). Industrial biocatalysis today and tomorrow. Nature *409*, 258–268. https://doi.org/10.1038/35051736.

6. Bell, E.L., Finnigan, W., France, S.P., Green, A.P., Hayes, M.A., Hepworth, L.J., Lovelock, S.L., Niikura, H., Osuna, S., Romero, E., et al. (2021). Biocatalysis. Nat. Rev. Methods Primers *1*, 46. https://doi.org/10.1038/s43586-021-00044-z.

7. Jakoblinnert, A., Mladenov, R., Paul, A., Sibilla, F., Schwaneberg, U., Ansorge-Schumacher, M.B., and de María, P.D. (2011). Asymmetric reduction of ketones with recombinant *E. coli* whole cells in neat substrates. Chem. Commun. *47*, 12230–12232. https://doi.org/10.1039/c1cc14097c.

8. Wittwer, M., Markel, U., Schiffels, J., Okuda, J., Sauer, D.F., and Schwaneberg, U. (2021). Engineering and emerging applications of artificial metalloenzymes with whole cells. Nat. Catal. *4*, 814–827. https://doi.org/10.1038/s41929-021-00673-3.

9. van Schie, M.M.C.H., Spöring, J.D., Bocola, M., Domínguez de María, P., and Rother, D. (2021). Applied biocatalysis beyond just buffers - from aqueous to unconventional media. options and guidelines. Green Chem. *23*, 3191–3206. https://doi.org/10.1039/d1gc00561h.

10. Kratzer, R., Woodley, J.M., and Nidetzky, B. (2015). Rules for biocatalyst and reaction engineering to implement effective, NAD(P)H-dependent, whole cell bioreductions. Biotechnol. Adv. *33*, 1641–1652. https://doi.org/10.1016/j.biotechadv.2015.08.006.

11. Dennig, A., Lülsdorf, N., Liu, H., and Schwaneberg, U. (2013). Regioselective o-hydroxylation of monosubstituted benzenes by P450. Angew. Chem. Int. Ed. *52*, 8459–8462. https://doi.org/10.1002/anie.

12. Ruff, A.J., Arlt, M., van Ohlen, M., Kardashliev, T., Konarzycka-Bessler, M., Bocola, M., Dennig, A., Urlacher, V.B., and Schwaneberg, U. (2016). An engineered outer membrane pore enables an efficient oxygenation of aromatics and terpenes. J. Mol. Catal. B Enzym. *134*, 285–294. https://doi.org/10.1016/j.molcatb.2016.11.007.

13. Tang, T.-C., An, B., Huang, Y., Vasikaran, S., Wang, Y., Jiang, X., Lu, T.K., and Zhong, C. (2021). Materials design by synthetic biology. Nat. Rev. Mater. *6*, 332–350. https://doi.org/10.1038/s41578-020-00265-w.

14. Wang, W., Yao, L., Cheng, C.Y., Zhang, T., Atsumi, H., Wang, L., Wang, G., Anilionyte, O., Steiner, H., Ou, J., et al. (2017). Harnessing the hygroscopic and biofluorescent behaviors of genetically tractable microbial cells to design biohybrid wearables. Sci. Adv. *3*, e1601984. https://doi.org/10.1126/sciadv.1601984.

15. Hu, Y., Rehnlund, D., Klein, E., Gescher, J., and Niemeyer, C.M. (2020). Cultivation of exoelectrogenic bacteria in conductive DNA nanocomposite hydrogels yields a programmable biohybrid materials system. ACS Appl. Mater. Interfaces *12*, 14806–14813. https://doi.org/10.1021/acsami.9b22116.

16. Srubar, W.V. (2021). Engineered living materials: Taxonomies and emerging trends. Trends Biotechnol. *39*, 574–583. https://doi.org/10.1016/j.tibtech.2020.10.009.

17. EIC Pathfinder Challenge: Engineered Living Materials. (2021). European Innovation Council, https://eic.ec.europa.eu/eic-funding-opportunities/calls-proposals/eic-pathfinder-challenge-engineered-living-materials_en.

18. Rodrigo-Navarro, A., Sankaran, S., Dalby, M.J., del Campo, A., and Salmeron-Sanchez, M. (2021). Engineered living biomaterials. Nat. Rev. Mater. *6*, 1175–1190. https://doi.org/10.1038/s41578-021-00350-8.

19. Lantada, A.D., Korvink, J.G., and Islam, M. (2022). Taxonomy for engineered living materials. Cell Rep. Phys. Sci. *3*, 100807. https://doi.org/10.1016/j.xcrp.2022.100807.

20. Daly, A.C., Riley, L., Segura, T., and Burdick, J.A. (2020). Hydrogel microparticles for biomedical applications. Nat. Rev. Mater. *5*, 20–43. https://doi.org/10.1038/s41578-019-0148-6.

21. Li, X., Sun, H., Li, H., Hu, C., Luo, Y., Shi, X., and Pich, A. (2021). Multi-responsive biodegradable cationic nanogels for highly efficient treatment of tumors. Adv. Funct. Mater. *31*, 2100227. https://doi.org/10.1002/adfm.202100227.

22. Correa, S., Grosskopf, A.K., Lopez Hernandez, H., Chan, D., Yu, A.C., Stapleton, L.M., and Appel, E.A. (2021). Translational applications of hydrogels. Chem. Rev. *121*, 11385–11457. https://doi.org/10.1021/acs.chemrev.0c01177.

23. Hawkins, K., Patterson, A.K., Clarke, P.A., and Smith, D.K. (2020). Catalytic gels for a prebiotically relevant asymmetric aldol reaction in water: from organocatalyst design to hydrogel discovery and back again. J. Am. Chem. Soc. *142*, 4379–4389. https://doi.org/10.1021/jacs.9b13156.

24. Li, X., Hetjens, L., Wolter, N., Li, H., Shi, X., and Pich, A. (2022). Charge-reversible and biodegradable chitosan-based microgels for lysozyme-triggered release of vancomycin. J. Adv. Res. https://doi.org/10.1016/j.jare.2022.1002.1014.

25. Liu, X., Inda, M.E., Lai, Y., Lu, T.K., and Zhao, X. (2022). Engineered living hydrogels. Adv. Mater. *34*, e2201326. https://doi.org/10.1002/adma.202201326.

26. Sun, J.Y., Zhao, X., Illeperuma, W.R.K., Chaudhuri, O., Oh, K.H., Mooney, D.J., Vlassak, J.J., and Suo, Z. (2012). Highly stretchable and tough hydrogels. Nature *489*, 133–136. https://doi.org/10.1038/nature11409.

27. Liu, X., Liu, J., Lin, S., and Zhao, X. (2020). Hydrogel machines. Mater. Today *36*, 102–124. https://doi.org/10.1016/j.mattod.2019.12.026.

28. Tang, T.C., Tham, E., Liu, X., Yehl, K., Rovner, A.J., Yuk, H., de la Fuente-Nunez, C., Isaacs, F.J., Zhao, X., and Lu, T.K. (2021). Hydrogel-based biocontainment of bacteria for continuous sensing and computation. Nat. Chem. Biol. *17*, 724–731. https://doi.org/10.1038/s41589-021-00779-6.

29. Hoffman, A.S. (2012). Hydrogels for biomedical applications. Adv. Drug Deliv. Rev. *64*, 18–23. https://doi.org/10.1016/j.addr.2012.09.010.

30. Connell, J.L., Kim, J., Shear, J.B., Bard, A.J., and Whiteley, M. (2014). Real-time monitoring of quorum sensing in 3D-printed bacterial aggregates using scanning electrochemical microscopy. Proc. Natl. Acad. Sci. USA *111*, 18255–18260. https://doi.org/10.1073/pnas.1421211111.

31. Anselmo, A.C., McHugh, K.J., Webster, J., Langer, R., and Jaklenec, A. (2016). Layer-by-layer encapsulation of probiotics for delivery to the microbiome. Adv. Mater. *28*, 9486–9490. https://doi.org/10.1002/adma.201603270.

32. Nguyen, P.Q., Courchesne, N.M.D., Duraj-Thatte, A., Praveschotinunt, P., and Joshi, N.S. (2018). Engineered living materials: prospects and challenges for using biological systems to direct the assembly of smart materials. Adv. Mater. *30*, e1704847. https://doi.org/10.1002/adma.201704847.

33. Lee, K.Y., and Mooney, D.J. (2012). Alginate: properties and biomedical applications. Prog. Polym. Sci. *37*, 106–126. https://doi.org/10.1016/j.progpolymsci.2011.06.003.

34. Teng, K., An, Q., Chen, Y., Zhang, Y., and Zhao, Y. (2021). Recent development of alginate-based materials and their versatile functions in biomedicine, flexible electronics, and environmental uses. ACS Biomater. Sci. Eng. *7*, 1302–1337. https://doi.org/10.1021/acsbiomaterials.1c00116.

35. Kearney, C.J., and Mooney, D.J. (2013). Macroscale delivery systems for molecular and cellular payloads. Nat. Mater. *12*, 1004–1017. https://doi.org/10.1038/nmat3758.

36. Ruff, A.J., Dennig, A., Wirtz, G., Blanusa, M., and Schwaneberg, U. (2012). Flow cytometer-based high-throughput screening system for accelerated directed evolution of P450 monooxygenases. ACS Catal. *2*, 2724–2728. https://doi.org/10.1021/cs300115d.

37. de Visser, S.P., and Shaik, S. (2003). A proton-shuttle mechanism mediated by the porphyrin in benzene hydroxylation by cytochrome P450 enzymes. J. Am. Chem. Soc. *125*, 7413–7424. https://doi.org/10.1021/ja034142f.

38. Whitehouse, C.J.C., Rees, N.H., Bell, S.G., and Wong, L.L. (2011). Dearomatisation of o-Xylene by P450(BM3) (CYP102A1). Chemistry *17*, 6862–6868. https://doi.org/10.1002/chem.201002465.

39. Melcrová, A., Pokorna, S., Vošahlíková, M., Sýkora, J., Svoboda, P., Hof, M., Cwiklik, L., and Jurkiewicz, P. (2019). Concurrent compression of phospholipid membranes by calcium and cholesterol. Langmuir *35*, 11358–11368. https://doi.org/10.1021/acs.langmuir.9b00477.

40. Clifton, L.A., Skoda, M.W.A., Le Brun, A.P., Ciesielski, F., Kuzmenko, I., Holt, S.A., and Lakey, J.H. (2015). Effect of divalent cation removal on the structure of gram-negative bacterial outer membrane models. Langmuir *31*, 404–412. https://doi.org/10.1021/la504407v.

41. Scholz, K.E., Okrob, D., Kopka, B., Grünberger, A., Pohl, M., Jaeger, K.E., and Krauss, U. (2012). Synthesis of chiral cyanohydrins by recombinant *Escherichia coli* cells in a micro-aqueous reaction system. Appl. Environ. Microbiol. *78*, 5025–5027. https://doi.org/10.1128/AEM.00582-12.

42. Wachtmeister, J., Jakoblinnert, A., and Rother, D. (2016). Stereoselective two-step biocatalysis in organic solvent: toward all stereoisomers of a 1, 2-diol at high product concentrations. Org. Process Res. Dev. *20*, 1744–1753. https://doi.org/10.1021/acs.oprd.6b00232.

43. Meyer, L.E., von Langermann, J., and Kragl, U. (2018). Recent developments in biocatalysis in multiphasic ionic liquid reaction systems. Biophys. Rev. *10*, 901–910. https://doi.org/10.1007/s12551-018-0423-6.

44. Mutti, F.G., and Kroutil, W. (2012). Asymmetric bio-amination of ketones in organic solvents. Adv. Synth. Catal. *354*, 3409–3413. https://doi.org/10.1002/adsc.201200900.

45. Sipponen, M.H., Farooq, M., Koivisto, J., Pellis, A., Seitsonen, J., and Österberg, M. (2018). Spatially confined lignin nanospheres for biocatalytic ester synthesis in aqueous media. Nat. Commun. *9*, 2300. https://doi.org/10.1038/s41467-018-04715-6.